Clays and Clay Minerals, Vol. 23, pp. 247–255. Pergamon Press 1975. Printed in Great Britain

NATURAL ALTERATION OF MICA AND REACTIONS BETWEEN RELEASED IONS IN MINERAL DEPOSITS

J. RIMSAITE

Geological Survey of Canada, 601 Booth Street, Ottawa, Ontario K1A OE8, Canada

(*Received* 3 *October* 1973)

Abstract—Chemical changes during the natural alteration of micas were studied by electron microprobe and classical chemical analyses of fresh and altered portions of mica flakes from 10 Canadian mineral deposits. Results of 50 new analyses are discussed in five examples, starting from simple changes in the interlayer followed by exsolution of titania and ending with complex replacements of anions and cations in all layers of the mica structure. Alteration of micas starts along 001 cleavage planes and fractures and gradually extends into the entire flake leaving some or no remnants of the host mica. The removal of ions from the mica structure and from the flake takes place by gradual depletion, by exsolution of oxides, and/or by alternating removal and redeposition of a newly-formed oxide, illustrated in the following example of the removal of Ti;

(1) removal of Ti from the mica structure and exsolution of rutile in the parent mica;

(2) destruction of rutile and recrystallization as anatase on the surface of the mica; and

(3) destruction of anatase, removal of Ti from the surface of the host and crystallization of anatase away from the parent mica.

Residual minerals replacing the original micas are secondary and recrystallized micas, chlorite, vermiculite, serpentine, talc and depleted, optically amorphous flakes. Newly-formed minerals which may incorporate the released ions into their structures are rutile, anatase, sericite, hydronepheline, chlorite-serpentine aggregates, goethite and jarosite. The following partly-altered micas are indicative of sulphide mineralization;

(a) bright-green, partly altered phlogopite from ultrabasic rocks and from Co–Cu–Fe–Ni sulphide assemblages. The green phlogopite formed by replacement of K, Al and Ti by Fe, Mg and OH;

(b) depleted mica coated with jarosite and Ni–goethite in the oxidation zone of a nickel deposit. The jarosite formed from released S and Fe from decomposed Fe–Ni sulphides and K released from the host mica; and

(c) chlorite–sericite–biotite alteration zones adjacent to Pb–Zn–Cu–Fe deposits.

INTRODUCTION

With increased information on proton losses from the mica structure in relation to controlled pH of solutions used in experimental alterations (Mehmel, 1938; Farmer *et al.*, 1971; Hoda and Hood, 1972; Robert and Pedro, 1972), it is interesting to compare the chemical trends of natural mica alteration. Micas are common hosts for ore minerals, and the mica layer adjacent to the ore is commonly altered to chlorite. The replacement of micas by ore minerals is in part mechanical, where ore minerals grow into and possibly promote the cleavage and fractures of mica (Fig. 1a) and/or chemical, where the silicate mineral is gradually replaced by ore minerals (Figs. 1b and 1f).

Electron microprobe and wet chemical analyses of fresh mica and its alteration products were carried out on about 50 minerals from 10 mineral deposits in an attempt to study natural alteration of micas in mineralized ultrabasic, alcalic and granitic rocks. The ultrabasic rocks from the three Cu–Ni deposits are partly to completely altered to serpentinites and characterized by low concentrations of Si, Al and alkalis, and the absence of feldspars. In these rocks, phlogopits is the principal carrier of Al and alkalis. Two deposits are at the contact between altered ultrabasic and granitic rocks, and two in alkalic rocks (a nepheline syenite and a syenite). Two sulphide deposits occur in granitic gneisses which contain mica bands in part replaced by Fe–Ni–Cu sulphides. In these deposits, micas adjacent to sulphides are altered to chlorite. One granitic gneiss contains disseminated Pb–Zn–Cu–Fe sulphides and is markedly altered to chlorite and kaolinite. The alteration of biotite (Fig. 1d) is probably hydrothermal, but some kaolinite might have formed under present or past weathering conditions. Three of the deposits contain prominent oxidized areas. The oxidized rocks vary from compact to crumbly fragments and dissintegrating gossan soils. Oxidation may have begun along fractures at depth during hydrothermal alteration and continued after exposure to surface weathering. All specimens studied are from compact Precambrian rocks collected mainly underground and from newly made exposures in the mining quarries.

SPECIMENS AND ANALYSES

Specimens

Polished thin sections of mica-bearing rocks from mineral deposits were examined under a petrographic

microscope and specimens containing partly altered micas were selected for electron microprobe analysis and for mineral concentration. Mica intergrowths and altered micas along rock fractures were separated from the remaining unaltered portions by crushing and hand-picking under the microscope. In coarse-grained specimens, the surface layer intergrown or coated with ore minerals was separated by cleaving with a razor blade and the ore minerals were separated from the mica layer by repeated crushing and screening. The ore minerals break more easily than the mica and were collected in the finest fraction, less than 30 μm dia. Final separation of different fresh mica species from the micas in various stages of alteration, and from flakes with adhering ore minerals was made in heavy liquids and with a Frantz isodynamic separator using procedures described by Rimsaite (1967b). All fractions of the concentrates were examined under a petrographic microscope and from several hundred "intermediate" fractions, two to five fractions having characteristic homogeneous optical properties and narrow ranges of specific gravity and magnetic susceptibility were chosen for x-ray and chemical analyses.

X-ray analyses

To determine the proportions of fresh mica and residual alteration products in partly altered samples, all concentrates were x-rayed with a Philips diffractometer using Ni-filtered Cu radiation at 45 kV and 16 mA on 001-oriented powder samples packed into shallow tray holders. Single-crystal Weissenberg photographs of fresh and altered portions of mica are also being made to determine structural changes.

Chemical analyses

Complete chemical analyses and partial analyses for H_2O, F, Cl, FeO and Fe_2O_3 were made of 17 fresh and altered micas using procedures described by Maxwell (1968).

Electron microprobe analyses

The homogeneity and distribution of selected elements in partly altered micas and in fine-grained alteration products were examined by electron scanning micrographs.

Selected elements in heterogeneous specimens were semi-quantitatively analysed using an energy dispersive spectrometer described by Lachance and Plant (1973). Total iron determined by an electron microprobe is reported as FeO. Water content, reported in brackets, was obtained by subtracting from 100 the sum of oxides determined by electron microprobe.

Tentative structural formulae

Most of the intermediate alteration products consist of sub-microscopic intergrowths or mixtures of fresh and altered minerals. The tentative structural formulae were calculated for the estimated fresh and altered components by subtracting proportions of the fresh component from the altered one and *vice versa*. x-ray powder diffraction results and/or potassium concentrations were used to estimate proportions of fresh mica in a partly altered specimen. The percentage of fresh mica component is given for each alteration product and was subtracted from the partly altered specimens before calculating structural formulae for the alteration products; thus 'A-30%F' indicates that 30% of fresh component 'F' was subtracted from the analysis to obtain the structural formula for the altered component 'A'. Because most specimens representing intermediate stages of alteration are submicroscopic mixtures of two or more structural phases, and because water in some specimens was not analysed, the structural formulae are tentative.

The structural formulae are based on 44 positive and negative charges (valencies) per unit cell for most micas, vermiculite and for tale, and on 56 valencies for residual chlorites. That some alteration products are probably mixtures of several phases, such as serpentine, talc, brucite and oxides, is evident from the excess of tetrahedral silicon and of octahedral contents in a few specimens.

Ionic percentages

Because micas and chlorites have different specific gravities and different numbers of cations and anions per unit cell, a direct comparison between these minerals cannot be made from their chemical analyses or structural formulae. The ionic percentages, however, provide the least distorted image of chemical trends during alteration reactions involving minerals with different crystal structures and show directly losses and gains of anions and cations in the interlayer, in the tetrahedral and octahedral layers, and in the O,OH-sheets. Examples of natural anionic and cationic changes during alteration of micas are given in Table 1. Tables containing electron microprobe analyses, structural formulas of micas and intermediate alteration products and calculated ionic proportions are available from the author upon request.

EXAMPLE I

Losses of interlayer cations and alteration of biotite to chlorite along 001-fractures

Specimens were collected from a brecciated oxidation zone in a Co–Ni deposit near the southeastern end of the Werner Lake, close to the Ontario–Manitoba boundary. The Werner Lake mining area, described by Carlson (1958), is in the Superior Province of the Canadian Shield. Massive and disseminated Fe–Cu–Co–Ni sulphides and cobaltite occur at the contact between serpentinized ultrabasic rocks and paragneisses and in brecciated zones. The low-temperature alteration, serpentinization, chloritization, and oxidation of these Archean rocks started probably under hydrothermal conditions, but the extensive oxidation and formation of gossans along rock fractures and disintegration of the oxidized fragments in the soil is attributed to weathering. The mineralized paragneiss selected for this study consists of quartz, gar-

Table 1. Examples of chemical changes during alteration of biotite.

	Example IIb RT-18 biotite Jarisite		Example IVa RM-10 biotite-sagenite-residual chlorite Sagenitic					Example V Phlogopite-vermiculite		
Weight (%)	Fresh (A)	coated (Y)	Fresh biotite A (C.A.)	(E.M.A.)	biotite B (E.M.A.)	Residual chlorite C (C.A.)	(E.M.A.)	Phlogopite (Ph)	Vermiculite (V)	Tale (T)
SiO_2	36·9	69·5	37·1	36·9	35·2	27·1	26·6	38·5	41·2	61·9
Al_2O_3	17·8	1·8	14·9	15·4	18·2	21·0	21·4	15·6	5·5	0·01
TiO_2	2·5	0·4	1·9	1·9	1·1	0·18	0·11	1·1	0·6	0·00
Fe_2O_3	2·0	7·5	3·2			1·71		0·0	0·0	0·7
FeO	13·8	2·9	13·7	(16·6)	(17·9)	13·6	(15·3)	5·2	3·1	0·6
MgO	13·0	2·0	13·3	13·7	18·0	23·5	23·9	23·2	37·0	33·0
MnO	0·2	0·0	0·15	0·14	0·13	0·13	0·16	0·1	0·02	0·02
Cr_2O_3	0·3	0·0	0·2			0·02		0·08	0·00	0·00
NiO	0·1	0·0	0·08			0·01		0·00	0·00	0·00
CaO	0·1	0·2	0·3	0·1	0·0	0·3	0·0	0·1	0·05	0·05
Na_2O	0·5	0·1	0·17	0·14	0·4	0·14	0·0	0·9	0·2	0·04
K_2O	9·6	0·6	8·9	9·6	5·7	0·08	0·0	8·8	3·0	0·00
H_2O	2·7	15·9	2·9		(3·4)	10·9		4·2	8·5	6·0
F	0·32	0·05	0·4		0·14*	0·1		1·3	0·5	0·07
Cl	0·01	0·05	0·2		0·16*	0·1		0·4	0·2	0·14
Rb ppm	500	40	230		93*	<30		750	300	<30
Sr ppm	<30	<30	13		11*	<30		110	30	<30

Chemical analysis, C. A., by J. L. Bouvier and J. G. Sen Gupta. Electron microprobe analysis, E.M.A. by G. R. Lachance.

* partial chemical analysis.

net, biotite, sericitized feldspar and disseminated Fe–Cu–Ni–Co sulphides and cobaltite which alter to purple patches of erythrite and bright red and yellow 'goethite' that crystallized in fractures, mainly along biotite. The rock has a streaky appearance due to parallel orientation of biotite flakes. In polished thin sections the biotite consists of alternating fresh bands 'A' and altered brown 'B', green 'C', and reddish 'D' bands of chloritized biotite along 001-fractures. Some of the altered biotite bands are rimmed and partly replaced by 'goethite' containing patches of fine-grained recrystallized chlorite 'E'. Plagioclase 'F' is almost entirely altered to sericite 'G' and locally replaced by secondary albite. Large garnets and quarts grains are fractures and the fractures coated with films of 'goethite', containing small remnants of chalcopyrite and cobaltite. The red hydroxides were identified by x-ray powder diffraction photographs as goethite, but as silica and other impurities were detected by microprobe analyses, the 'goethite' is written in quotation marks.

The results indicate that the alteration of biotite in bands 'B' and 'C' involved hydration and considerable losses of alkalis from the interlayer (from 8·5 to 0·4% K_2O), and of TiO_2 (from 2·9 to 0·9%), with lesser losses of Mg and Cr. Changes in concentrations of the other constituents are less than 10 per cent. The residual alteration products in brown 'B' and green 'C' bands are similar in chemical composition to the fine-grained chlorite 'E'. The bright red color of band 'D' is attributed to its higher Ti content (4·5% TiO_2). Structural formulae of fresh biotite 'A', residual chlorite 'C', and newly-formed sericite 'G' are as follows:

'A': $(Si_{5·5}\ Al_{2·5})\ (Al_{0·7}\ Ti_{0·3}\ Fe_3\ Mg_{1·6}\ Cr_{0·03})\ (Na_{0·1}\ K_{1·7})\ (OH)_4\ (O)_{20}$;

'C': $(Si_{7·2}\ Al_{0·8})\ (Al_{3·6}\ Ti_{0·04}\ Fe_{4·9}\ Mg_{1·8}\ Cr_{0·02})\ (OH)_{19}\ (O)_{18·5}$;

'G': $(Si_{6·5}\ Al_{1·5})\ (Al_{3·5}\ Ti_{0·01}\ Fe_{0·2}\ Mg_{0·08})\ (Na_{0·22}\ K_{1·6})\ (OH)_{3·4}\ (O)_{20·3}$.

The residual chlorites contain relatively high Al/Mg (1·8–2·35) and Fe/Mg (2·4–2·7) ratios in the octahedral layers. The sericite is phengitic and contains more Ti, Fe, Mg and K than the host plagioclase 'F' and secondary albite 'H'. The altered plagioclase has more Ca and K than the secondary albite.

EXAMPLE IIa, b, c, d, e

Incorporation of iron into micas and their alteration products

Micas are frequent hosts for secondary oxides, and some iron can apparently be fixed in the interlayer of partly-chloritized micas. Examples IIa and IIb are on alteration of micas under iron oxide coatings and on their replacement by oxides. Examples IIc, IId and IIe summarize results obtained on bright-green partly altered micas and chlorites formed from phlogopites by addition of iron in serpentinites.

IIa. Decomposition of phlogopite under hematite crusts. Coarse-grained phlogopite crystals coated with hematite plates were collected in an abandoned hematite mine, located in Precambrian metamorphosed limestones about 10 miles north of Ottawa Fresh phlogopite 'A' (without oxide inclusions) and the hematite-coated surface layer 'B' were separated for complete chemical analyses. The concentrate of fresh phlogopite was clean, but concentrate 'B' contained adhering fresh phlogopite, 8 per cent hematite and about 2% calcite and chert. Phlogopite, hematite and calcite in the hematite-coated chlorite layer 'B' were identified on x-ray diffraction patterns. Analytical results and structural formulae of fresh phlogopite 'A': $(Si_{5·8}\ Al_{2·2})\ (Al_{0·1}\ Ti_{0·1}\ Fe^{3+}_{0·2}\ Fe^{2+}_{0·55}\ Mg_{4·8}\ Mn_{0·03}\ Li_{0·06})\ (Ca_{0·03}\ Na_{0·08}\ K_{1·83})\ (OH_{2·03}\ F_{1·33})\ (O)_{20·3}$ and of altered layer 'B': $(Si_7Al_1)\ (Al_{1·2}\ Ti_{0·05}\ Fe^{3+}_{0·4}\ Fe^{2+}_{1·4}\ Mg_{8·5}\ ^{Mn}_{0·02}\ Li_{0·1})\ (OH_{17·6}\ F_1)\ (O)_{19·4}$, indicate the following losses from the chloritized surface layer 'B'; (a) total removal of interlayer cations, K and Na (b) 50–75% losses of Ti from the octahedral layer and of F from the O,OH-sheets and (c) 50%

or less losses of Rb from the interlayer, and of Si and Al from the tetrahedral layer. The altered surface layer gained water, iron and apparently some magnesium. The hematite-rich crusts contain 50 per cent more Ni and Zn than the host mica. This example provides evidence of the removal of cations from the interlayer and from the tetrahedral and octahedral layers, accompanied by an apparent increase of Fe and Mg, and on the loss of fluorine from the O,OH-sheets during alteration of phlegepite under the hematite crust. The replacement of the phlogopite by hematite started on the surface and along the 001 cleavage planes. Mechanical separation of the two minerals is not possible. The strong adherence of the iron oxide (or hydroxide) to the surface of chloritized mica layer may be mechanical and/or chemical, and may possibly involve ionic bonding between their surface layers.

IIb. Alteration of biotite under jarosite and 'Ni-goethite' crusts. Mineralized biotite-rich layers in schists of the Thompson Nickel Belt, Manitoba, (Zurbrigg, 1963), provide an interesting example of alteration of biotite to optically-amorphous flakes and of biotite replacement by jarosite and 'Ni-goethite' (Fig. 1f, RT-18). In fresh portions of the rock, the biotite is entirely fresh ('A' in Table 1); only in oxidized portions of the rock does the biotite exhibit various degrees of alteration, thereby suggesting that decomposition and oxidation of sulphides and alteration of the biotite are related. In oxidized areas of the schist, the biotite consists of alternating fresh and altered bands, locally replaced by 'goethite' and jarosite. Small tablets and specks of jarosite (1–3 μm dia.) crystallized on the surface and along basal cleavage planes of the altered biotite. Some of the biotite flakes have undergone almost complete structural destruction; they appear discoloured and amorphous under the microscope. Chemical analysis (Table 1, RT-18 'Y') of the amorphous flakes indicates apparent enrichment of SiO_2 (about 70 per cent), and depletion of the other constituents. Single-crystal Weissenberg patterns, x-rayed 500 hr, contain very weak (221)-reflections inferring strctural destruction of the altered flakes.

The destruction and replacement of biotite in the schist has taken place in stages. At the initial stage of alteration, the biotite consists of bright (fresh) and dark (altered) bands, with the latter coated or replaced by 'goethite'. The 'goethite' contains 14% SiO_2, 4% Al_2O_3, and 1–8% Ni adjacent to the remnant biotite (Rimsaite, 1973a). The jarosite retains most of the potassium (8% K_2O) and 50% of the rubidium (300 ppm) released from the altered biotite host. The replacement of biotite by jarosite and 'Ni-goethite' starts at the surface and along fractures of the biotite gradually spreading into adjacent portions of a flake till the mica is entirely replaced by clastic jarosite–'goethite' aggregates. The altered rock crumbles to small fragments and disintegrates in the soil. The bright yellow and red patches in the disintegrating rock and soil, and red-stained areas with oxide-coated mica bands at the surface are good indicators of the occurrence of sulphide mineralization below the surface.

IIc. Iron-rich coatings on the surface of phlogopite, and incorporation of the iron into the interlayer of residual chlorite. The adsorbed and/or bonded hydroxides on the surface and between the 001 cleavage planes of K-depleted micas are of great interest in connection with the crystallization of iron-rich chlorites. The iron hydroxides apparently can be fixed in the interlayer of the altered mica to form chlorite with higher iron contents than that in the host mica.

Specimen R-Co-7, from the oxidation zone of the Co–Ni deposit discussed in Example I, was collected at the contact between a paragneiss and a mineralized basic rock. In this contact rock, the original olivine is entirely replaced by serpentine and very fine-grained magnetite; small remnants of pyroxene are enclosed in hornblende, and coarse-grained phlogopite with green chloritized edges is in part replaced and surrounded by acicular chlorite–serpentine–talc aggregates. The rock is brecciated and contains disseminated sulphides and a few patches of coarse-grained calcite and tremolite. A few bright-green Al-spinels enclose phlogopite flakes partly altered to chlorite. 'Goethite' crystallized along 001 planes of some micas. The purposes of the electron microprobe analysis was to determine chemical trends during metamorphic alteration of phlogopite 'A' to the following residual chlorites:

'C' = depleated, chloritized phlogopite under 'goethite' coatings;

'D' = green chloritized edges of the phlogopite adjacent to chlorite–serpentine–tale aggregates, formed in Mg–Fe-rich environment;

'E' = chloritized phlogopite enclosed in Al-spinel, formed in Al-rich environment;

'F' = acicular flakes of chlorite-tale adjacent to sulphides. Structural formulae of the original phlogopite and of residual alteration products show chemical differences depending on diverse environments of crystallization. The fresh phlogopite 'A': $(Si_{5.2}\ Al_{2.8})$ $(Al_{0.5}\ Ti_{0.1}\ Fe_{0.8}\ Mg_{4.7}\ Mn_{0.01})$ $(Ca,Na_{0.08}\ K_{1.86})$ $(OH)_{3.8}$ $(O)_{20.1}$ contains relatively low Si/Al ratio in the tetrahedral layer thereby reflecting low concentration of silica in the host ultrabasic rock. The chlorite component 'C' under the 'goethite' crust, 'C' = $(Si_{5.8}\ Al_{2.2})$ $(Al_{2.7}\ Ti_{0.1}\ Fe_1\ Mg_8\ Mn_{0.1})$ $(OH)_{16}$ $(O)_{20}$ contains a smaller ionic proportion of Si and more Mg and Mn than the host phlogopite. When the 'goethite' coating is included in the structural formula, iron contents of the chlorite components 'C', 'D' and 'E' are similar and about twice as high as the iron content in the host phlogopite 'A'. Iron hydroxides precipitate either as 'goethite' coatings on the surface of the phlogopite ('C'), or are fixed in the interlayer of the K-depleted phlogopite to form green chloritized edge 'D'. Structural formula for chlorite component 'D': $(Si_6\ Al_2)$ $(Al_{1.1}\ Fe_{3.4}\ Mg_{6.1}\ Mn_{0.2})$ $(OH)_{20}$ $(O)_{18}$ indicates a marked increase of iron and manganese. The residual chlorite 'E' crystallizes in Al–

Cr environment. It has a relatively high Al-content, similar to that in chlorite 'C', and 0·3% Cr in the structure. The Al-content decreases in green chloritized edges of the phlogopite, reaching the lowest concentration in the acicular flakes 'F' which are intergrown with sulphides. Structural formulae calculated on the basis of 56 and 44 valencies indicate unusual composition of the tetrahedral layer of flakes 'F', inferring the presence of chlorite-talc intergrowths in about equal proportions of the two components. Structural formula for talc component 'F': (Si_8) $(Fe_{1\cdot2}$ $Mg_{4\cdot6})$ $(OH)_{5\cdot3}$ $(O)_{19\cdot3}$ indicates the presence of iron in the talc structure which crystallized in an iron-rich environment adjacent to pyrrhotite. The Example IIc illustrates that chemical trends during alteration of mica at the contact between basic and granitic rocks, and compositions of residual chlorites depend on locally prevailing environmental conditions.

IId. Partly altered bright-green phlogopites in mineralized ultrabasic rocks from Ni-*deposits.* Bright-green, partly chloritized phlogopites occur in association with pyrrhotite–pentlandite ore in Marbridge (Quebec) and in Werner Lake (Ontario) Cu–Ni deposits, and in serpentinized ultrabasic rocks of the Thompson Nickel Belt (Manitoba). Because of their frequent association with Fe–Ni sulphides, the green partly altered phlogopites are believed to be indicative of Fe–Ni mineralization. In the serpentinized ultrabasic rocks, which are characterized by low concentrations of Al and Si, phlogopite is the sole primary rock-forming mineral containing alumina and alkalis.

Green phlogopites with K-deficient chloritized edges in specimen TH-875 are enclosed in fine-grained serpentine-chlorite-talc aggregates which contain less Al than the chlorite-serpentine-talc groundmass in a contact rock of Example IIe. Although the iron content increases in all green partly altered phlogopites, the intermediate phase of 'goethite'-coated flakes was not observed in phlogopites TH-875. Fresh phlogopite 'A', its green, chloritized portions 'B', and chlorite-talc pseudomorphs 'C' contain similar concentrations of silica, but Al, Ti, Cr and K contents markedly decrease from 'A' to 'C', whereas Fe and Mg contents increase. Tentative structural formulae for specimen 'B' were calculated as for mica and as for chlorite, after subtracting 60 per cent of the fresh component 'A'. The proportions of fresh mica and chlorite were estimated from x-ray diffraction patterns by measuring the intensity ratios of their basal reflections (Rimsaite, 1967b). The residual alteration product 'C' contains very little Al_2O_3 (1·2%) and its structural formula was calculated as for 'talc', after subtracting 15 per cent of chlorite component 'B'. The fresh phlogopite 'A' is characterized by low Si/Al ratio; $(Si_{5\cdot2}$ $Al_{2\cdot8})$ $(Al_{0\cdot29}$ $Ti_{0\cdot1}$ $Fe_{0\cdot4}$ $Mg_{5\cdot7}$ $Cr_{0\cdot1}$ $Ni_{0\cdot01})$ $K_{1\cdot5}$ $(OH)_{3\cdot3}$ $(O)_{19\cdot8}$. The phlogopite from the ultrabasic rock associated with Ni deposits contains Cr and Ni in the structure and this is released during its alteration. The bright-green edges 'B' contain less K, Al, Ti and Cr, and more OH, Fe and Mg than the host phlogopite. Because of the marked decreases in Al-contents (from 17·8 to 1·2% Al_2O_3 in 'C'), the green edges 'B' and the ultimate alteration product chlorite–talc 'C' contain insufficient Si and Al to fill the tetrahedral positions: $(Si_{5\cdot5}$ $Al_{2\cdot4}$ $Ti_{0\cdot06}$ $Fe_{0\cdot04})^{IV}$ $(Fe_{0\cdot7}$ $Mg_{6\cdot1}$ $Cr_{0\cdot06}$ $Ni_{0\cdot01})$ $K_{1\cdot1}$ $(OH)_5$ $(O)_{19\cdot5}$ in green, depleted phlogopite edges calculated as 'mica', and in the chlorite component 'B' of the same green edges, calculated as 'chlorite': $(Si_7$ $Al_1)$ $(Al_{2\cdot4}$ $Ti_{0\cdot07}$ Fe_1 $Mg_{8\cdot2}$ $Cr_{0\cdot07}$ $Ni_{0\cdot01})$ $(OH)_{15}$ $(O)_{20\cdot5}$. The structural formula calculated as chlorite for specimen 'C' has also unusual composition of the tetrahedral layer: $(Si_{7\cdot1}$ $Al_{0\cdot3}$ $Fe_{0\cdot6})^{IV}(Fe_{0\cdot3}$ $Mg_{12\cdot4})$ $(OH)_{13\cdot6}$ $(O)_{21\cdot2}$.

IIe. Reactions indicating removal of silica at the initial stages of alteration followed by relative increases at advanced stages of alteration. Serpentinite TH-866 from the Thompson Nickel Belt, Manitoba, was chosen to show variations in the concentration of silica with advancing stages of alteration. The bright-green chloritized phlogopite is associated with Fe–Ni sulphides in the serpentinized ultrabasic rock. This mica exibits trends of alteration similar to those in Example IIe. The Mg increases from 27 per cent in fresh mica 'A' to 44·7% in residual alteration product 'D' with decreasing Al, from 14·4% in 'A' to 0·2% in 'D'. However, mica and its alteration products in TE-866 differ in the composition of the tetrahedral layer and in the marked decrease of the silica content in the green chloritized edge 'B' (from 39% in 'A' to 30% in 'B'). The fresh phlogopite 'A' and the residual alteration products 'B', 'C' and 'D' contain insufficient Si and Al to fill the tetrahedral positions. The green color of the chloritized edge 'B' is attributed to its greater Fe and OH contents, decrease of Ti, and to Fe_2O_3/FeO being >1. Although the Si content increases in talc 'D', Al is almost absent, thus part of Mg and all Ti and Fe were placed in the tetrahedral layer to fill the vacant positions. Three possibilities are suggested to account for the unusual compositions of the tetrahedral layer of the sheet silicates in the ultrabasic rocks:

(1) the tetrahedral layer has unusual composition: $Si_{5\cdot84}$ $Al_{0\cdot04}$ $Fe_{0\cdot66}$ $Mg_{1\cdot46}$ in RT-866 'D';

(2) the tetrahedral layer may have unoccupied positions, and the total charge (valencies) might have changed;

(3) additional phases, such as brucite and other oxides and hydroxides are present.

The suggested possibilities warrant special x-ray and electron microscope studies.

The chlorite 'C' has unusual composition of both tetrahedral and octahedral layers, with a marked deficiency of Al and excess of Mg that infers the presence of brucite in sub-microscopic intergrowths. The uncommon Al-poor chlorites and Fe-rich talc varieties observed in the mineralized ultrabasic rocks also warrant more detailed analyses. The ultrabasic rocks studied have no secondary minerals which could accommodate the K released from the altered phlogopite.

EXAMPLE III

Transition of biotite to lepidomelane by replacement of octahedral Al, Ti *and* Mg *by* Fe, *and secondary micaceous alteration products in a nepheline deposit.*

Brown biotite, green lepidomelane with variable Mg-contents and their oxidation products have already been described by Rimsaite (1967a) and by Farmer *et al.* (1971). Later electron microprobe analyses of the biotite and lepidomelane indicated local variations in Mg-contents, resulting from remnants of brown Mg-bearing biotite. A new lepidomelane concentrate, containing less than 0·1% MgO, was prepared for chemical analysis. The lepidomelane forms from biotite by gains of iron, as do the green Fe-rich chloritized edges and bands in phlogopite discussed in Example II. In the lepidomelane, however, replacement of Al, Ti and Mg takes place in the octahedral layer without alteration to chlorite.

Origin of lepidomelane. The lepidomelane occurs as black to dark green coarse crystals containing magnetite inclusions surrounded by secondary albite in a nepheline syenite (Fig. 1e). The difference in iron content between the early brown biotite 'A' and late lepidomelane 'B' resembles that between green chloritized mica edges and their host phlogopite. The presence of iron during crystallization of the iron-rich micas is inferred by the association with magnetite and with Fe–Ni sulphides. Structural formulae of biotite 'A': $(Si_5\ Al_3)\ (Al_1\ Ti_{0\cdot23}\ Fe^{3+}_{0\cdot4}\ Fe^{2+}_{2\cdot1}\ Mg_{1\cdot9}\ Mn_{0\cdot08})\ (Ca,Na_{0\cdot07}\ K_{1\cdot82})\ (OH_{2\cdot88}\ F_{0\cdot2}\ Cl_{0\cdot2})\ O_{20\cdot6}$ and of lepidomelane 'B' $(Si_{5\cdot2}\ Al_{2\cdot8})\ (Al_{0\cdot7}\ Ti_{0\cdot07}\ Fe^{3+}_{0\cdot7}\ Fe^{2+}_{4\cdot2}\ Mg_{0\cdot01}\ Mn_{0\cdot11})\ (Ca_{0\cdot01}\ K_{1\cdot9})\ (OH_{3\cdot3}\ F_{0\cdot07})\ O_{20\cdot3}$ indicate significant replacements in the octahedral layer; iron and Mn increase at the expense of Al, Mg and Ti. Changes in the OH,O-sheets are also important: the newly-formed lepidomelane contains little fluorine and no chlorine, in contrast to the early biotite which contains relatively abundant F and Cl. The occupancy of the interlayer does not change much, but lepidomelane loses Na and gains Rb (0·04% in 'A' and 0·7% Rb_2O in 'B'). Unlike bright-green oxidized edges in Example II, the lepidomelane has a deficient hydroxyl group, resulting probably from oxidation of ferrous iron at the expense of hydroxyl. However, it is possible that the Fe^{3+} replaces Al^{3+} in the octahedral layer; therefore the structural formula of the lepidomelane was based on 44 valencies, assuming that the total number of (±) charge did not change.

Oxidation of lepidomelane. Oxidized lepidomelane 'C' formed on the surface and along basal cleavage planes of the host mica. The oxidized ferric lepidomelane shows similar variations in Mg-contents as those observed in the parent lepidomelane. The concentrate prepared for analysis contained only 0·1% MgO, and its x-ray diffraction patterns indicated no chlorite or vermiculite impurities. However, broad basal reflections on x-ray single-crystal Weissenberg patterns, possibly due to *ca.* 2 per cent 'strongly adsorbed water', determined by TG and i.r. analyses, suggest that the oxidized lepidomelane 'C' might represent a transition phase between mica and an expanded mineral, such as chlorite or vermiculite. The oxidized lepidomelane 'C' has almost all ferrous oxide oxidized to ferric oxide, which increases the positive charge in the octahedral layer, thereby reducing the resulting negative charge of the tetrahedral and octahedral layers. Partial loss of the K apparently results from the increased positive charge of the octahedral layer. The oxidized lepidomelane retains the single-layer monoclinic structure of the host lepidomelane 'B'. Compared with the three-layer rhombohedral oxidized biotite described as an 'intermediate mica' by Rimsaite (1967a), lepidomelane 'B' and its oxidation product 'C' have a different crystal structure, and less MgO. The structural formula for the oxidized lepidomelane 'C' was based on '$44 + z$' = 47 valencies, where '$+z$' was determined from the charge difference between the original lepidomelane 'B' and oxidized portion 'C' (Rimsaite, 1970). Although the lepidomelane has local magnetite and albite inclusions (Fig. 1e), clean and homogeneous concentrates 'B' and 'C' were obtained by careful electromagnetic and heavy liquid separations, followed by repeated optical and x-ray examination of concentrates during their preparation. It is believed that the increase in valencies '$+z$' is real resulting mainly from oxidation of iron, whereby the structural formula based on 47 valencies for the oxidized lepidomelane represents this rare mineral without distortion: $(Si_{5\cdot2}\ Al_{2\cdot8})^{IV}(Al_{0\cdot6}\ Ti_{0\cdot05}\ Fe^{3+}_{4\cdot6}\ Fe^{2+}_{0\cdot06}\ Mg_{0\cdot1}\ Mn_{0\cdot1})^{VI}(Ca_{0\cdot1}\ K_{1\cdot4})\ (OH)_{3\cdot5}\ O_{21}\ (H_2O)_{0\cdot5}$.

Secondary micaceous minerals in a nepheline deposit

Most of the nepheline crystals are partly to completely altered to fine-grained secondary minerals: muscovite-sericite, 'hydronepheline', zeolites and a fine-grained aggregate composed of chlorite–serpentine–mica intergrowths, commonly referred to as 'gieseckite'. Some of these secondary minerals are submicroscopic in size; others are 40 μm in diameter. The secondary minerals also crystallize in cavities and fractures. Biotite flakes partly altered to chlorite have been discussed by Rimsaite (1967a). Textural relationships suggest at least three periods of crystallization of the secondary sheet silicates.

Sericite. Sericite flakes, about 40 μm in diameter, replace host nepheline along the fractures. The fine-grained sericite 'E', concentrated from a nepheline host, differs from the coexisting primary coarse-grained muscovite 'D' by lesser Mg, F and Cl contents, and by slightly higher concentration of ferrous iron, as can be seen from their structural formulae: 'D' = $(Si_6\ Al_2)\ (Al_{3\cdot7}\ Fe^{3+}_{0\cdot24}\ Fe^{2+}_{0\cdot26}\ Mg_{0\cdot03})\ (Na_{0\cdot15}\ K_{1\cdot75})\ (OH_{3\cdot9}\ F_{0\cdot06}\ Cl_{0\cdot05})\ O_{20}$, and 'E' = $(Si_{5\cdot9}\ Al_{2\cdot1})\ (Al_{3\cdot7}\ Fe^{3+}_{0\cdot23}\ Fe^{2+}_{0\cdot13}\ Mg_{0\cdot01})\ (Ca_{0\cdot03}\ Na_{0\cdot19}\ K_{1\cdot75})\ (OH_{4\cdot7}\ F_{0\cdot04})\ O_{19\cdot6}$.

'*Hydronepheline*'. Hydronepheline is a fine-grained aggregate of sericite–analcite intergrowths, identified in x-ray powder diffraction patterns. The particle size is less than 2 μm, visible under an electron microscope

using magnification × 60,000. The 'hydronepheline' is an alteration product of nepheline, but locally it replaces all earlier-formed minerals, including feldspar and secondary sericite. Areas replaced by 'hydronepheline' have a pink, patchy appearance. The hydronepheline 'F' differs from sericite 'E' and muscovite 'D' by lesser Fe, Al and K contents and higher Mg, Na and H_2O contents. Higher concentration of Na is accounted for by the presence of analcite, and CaO is contained in calcite impurities. The excess H_2O in the fine-grained micaceous minerals is a 'strongly adsorbed water' which remains after heating at 110°C and was studied in some detail by DTA, TGA and i.r. analyses. The analcite (15%) and CaO were subtracted from chemical analysis before calculating the structural formula for the mica component of the 'hydronepheline':

$$(Si_6\ Al_2)\ (Al_{3\cdot9}\ Fe^{3+}_{0\cdot03}\ Fe^{2+}_{0\cdot03}\ Mg_{0\cdot2})$$
$$(Na_{0\cdot19}\ K_{1\cdot7})\ (OH_{3\cdot97}\ F_{0\cdot01})\ O_{20}$$
$$(\text{adsorbed } H_2O = 0\cdot5).$$

Replacement of nepheline 'H' by sericite 'E' and by hydronepheline 'F' results in the release of sodium which has crystallized in secondary minerals, analcite, zeolites and in secondary albite 'I' that surrounds magnetite crystals in lepidomelane 'B'.

Fine-grained chlorite-serpentine-mica aggregates ('gieseckite') 'G'. These very fine-grained (sub-microscopic) aggregates produce very poor x-ray powder diffraction patterns of chlorite-serpentine and mica. A fibrous variety of the aggregates crystallizes along fractures and joints in the nepheline syenite, and massive aggregates replace nepheline, feldspars, biotite, muscovite and other minerals producing greenish-grey alterations in the host rock. The greenish, altered patches vary in size from a few millimeters to a few centimeters and locally may constitute more than 50 per cent of the rock. It is interesting to point out that the fine-grained micaceous alteration products, and the metasomatic lepidomelane, do not fix the released anions, F and Cl, and contain mainly hydroxyl in the OH,O-sheets. Structural formula was calculated for the chlorite component 'G' after subtracting estimated 5 per cent nepheline and 15 per cent muscovite:

$$(Si_{6\cdot4}\ Al_{1\cdot6})\ (Al_{3\cdot75}\ Fe^{3+}_{0\cdot3}\ Fe^{2+}_{1\cdot7}\ Mg_6)$$
$$(OH_{15}\ F_{0\cdot02}\ Cl_{0\cdot02})\ O_{20\cdot5}.$$

The following sequence of crystallization of micaceous alteration products was observed in the nepheline deposit:

(1) brown biotite 'A' releases Mg, Al, Ti, F and Cl and alters to lepidomelane which gains Fe and OH;

(2) nepheline 'H' alters to sericite 'E' and subsequently to hydronepheline 'F' and releases sodium;

(3) the released sodium can be accounted for in part by the presence of secondary Na-bearing minerals, analcite, zeolites and secondary albite 'I' which replace primary minerals and form in interstices surrounding magnetite in lepidomelane;

(4) chlorite-serpentine-mica aggregates 'G' crystallize in rock fractures and replace nepheline syenite in irregular patches thereby producing a peculiar spotted greenish-grey alteration of the rock.

EXAMPLE IV

Alteration of biotite in granitic rocks containing quartz and sulphides

Alteration of biotite in Si-Al-rich rocks is different from that observed in Si-deficient, ultrabasic rocks. In the Al–Si-rich rocks affected by low temperature metamorphism or hydrothermal alteration, biotite alters to Al-rich chlorite by losing K, Si and Ti and gaining Al. At the initial stage of alteration, the titania exsolves as rutile needles (Rimsaite, 1973b, Fig. 12) and the biotite changes in color from brown to green. Chemical changes during three stages of alteration were studied on fresh and chloritized biotites in altered meta-greywacke from Marbridge nickel deposit, Quebec (Example IVa). The K released from the biotite structure is either removed from the site or it can be fixed in the secondary muscovite which replaces biotite (Fig. 1d). The muscovite which is formed by replacement of biotite contains brown patches of remnant altered biotite and is usually phengitic.

Example IVa. Fresh and altered biotites in various degrees of chloritization were concentrated from metamorphosed greywacke RM-10 collected in Marbridge No. 2 nickel deposit, Quebec. General geology and distribution of the greywacke are discussed by Dawson (1966, Map 1179A), and mine geology is described by Buchen and Blowes (1968). The meta-greywacke consists of alternating biotite–chlorite and quartz–plagioclase bands, and contains disseminated pyrite. The rock is altered along fractures. Crenulated zig-zag veinlets of chlorite in biotite can be seen in Fig. 1(c). With advanced alteration, chloritization spreads into the biotite bands.

Results of chemical and electron microprobe analyses are compared in Table 1, RM-10, include those of fresh biotite 'A'. Partly altered biotite with exsolved rutile 'B' was analysed by an electron microprobe, and almost entirely chloritized biotite 'C' with a few rutile needles, and green chlorite without rutile by wet chemical analysis. Considering that electron microprobe analyses were made in polished thin sections on small areas, representing only a few square microns of a flake and chemical analyses were made on concentrates containing many thousands of mica flakes representing different stages of alteration, the analyses compare remarkably well and show definite chemical trends with progressive alteration. The chlorite and biotite proportions in partly altered micas were calculated from their x-ray powder diffraction charts. The results in Table 1 show gradual decreases for K, Ti, Si, F and Cl, differential losses of

Rb and Sr, and increases of Al and Mg. It is interesting to point out that during hydration, the fluorine is apparently less stable in the mica structure than the chlorine.

Example IVb. Alteration of biotite in a kaolinitized gneiss. Replacement of biotite by Mg–Fe–Al *chlorites and muscovite.* In the altered gneiss R-Kp-5, biotite is almost entirely altered to chlorite. A few remnants of fresh biotite are preserved in quartz and a few patches of altered biotite remain in muscovite which replaces the biotite (Fig. 1d). Electron microprobe analyses of fresh biotite 'A', enclosed in quartz; of altered biotite remnant 'B' in muscovite; of Mg-rich 'C', Fe-rich 'D' and Al-rich 'E' chlorites; and of muscovite 'M' indicate the following chemical trends: during alteration of biotite to Mg-rich chlorite ('A' to 'C'), the K, Si, Ti, Mn and Fe decrease, while Al and Mg apparently increase. Deep-green chlorite 'D' is most abundant and shows similar chemical trends, but contains less Mg and more Fe than chloritized biotites 'B' and 'C', whereas chlorite 'E' contains much more Al_2O_3 (27%) and about ten times less iron (1·8% FeO) than the Fe-rich chlorite 'D' (18·4% Al_2O_3 and 26·1% FeO). The muscovite 'M' replaces biotite whereby the Ti, Fe, Mg and Mn are removed from the biotite and substituted by Si, Al, Na and K in the muscovite structure. During the replacement of biotite by muscovite, the biotite is a host and in part a supplier of the Al, Si and K, but ionic proprotions change in the interlayer (higher proportion of Na), in the tetrahedral layer (higher Si/Al ratio) and in the octahedral layer of the muscovite, as can be seen from the following structural formulae:

biotite 'A': $(Si_{5.7}\ Al_{2.3})\ (Al_{0.1}\ Ti_{0.4}\ Fe_{2.9}\ Mg_{2.2}\ Mn_{0.03})\ (K_{1.72})\ (OH)_{4.7}\ (O)_{19.6}$;

Mg-rich chlorite 'C': $(Si_{5.6}\ Al_{2.4})\ (Al_{2.1}\ Ti_{0.04}\ Fe_{3.3}\ Mg_{6.7}\ Mn_{0.02}\ Cr_{0.01})\ (OH)_{16}\ (O)_{20}$;

Fe-rich chlorite 'D': $(Si_{5.5}\ Al_{2.5})\ (Al_{2.3}\ Ti_{0.04}\ Fe_{4.9}\ Mg_{4.8}\ Mn_{0.04}\ Cr_{0.02})\ (OH)_{22}\ (O)_{17}$;

Al-rich chlorite 'E': $(Si_{6.4}\ Al_{1.6})\ (Al_{4.8}\ Fe_{0.3}\ Mg_{5.3})\ (OH)_{27}\ (O)_{15}$;

Muscovite 'M': $(Si_{6.5}\ Al_{1.5})\ (Al_{3.6}\ Ti_{0.01}\ Fe_{0.12}\ Mg_{0.43})\ (Na_{0.18}\ K_{1.66})\ (OH)_{3.5}\ (O)_{20.3}$.

The muscovite 'M' and Al-rich chlorite 'E' are the least abundant alteration products of biotite in the gneiss R-Kp-5. Chemical differences between the residual alteration products replacing the biotite are attributed to the local distribution and availability of the particular ions during the alteration. Alteration of biotite to Al–Mg-rich chlorite is related to the alteration of feldspars which are replaced by fine-grained quartz, minor chlorite and kaolinite thereby releasing alkalis and alumina.

EXAMPLE V

Natural alteration of phlogopite to vermiculite and talc

Specimens of coarse-grained phlogopite, slightly to markedly altered to vermiculite and to talc on slickenside surfaces were collected in the Olympus vermiculite mine, Ontario. The phlogopite–vermiculite veins, containing commercial vermiculite, transect altered syenite rocks. The phlogopite was separated from the vermiculite host where it occurs as discrete remnants. It contains about 10 per cent of vermiculite 'V' which was estimated from x-ray diffraction patterns using the procedure described by Rimsaite (1973, Fig. 10). The vermiculite concentrate 'V' contains about 30 per cent of phlogopite component 'Ph' which was subtracted before calculating the structural formula. Talc 'T' retains the general habit of phlogopite–vermiculite but under a microscope it is seen to be composed of fine particles, arranged in parallel rows and contains specks of magnetite and hematite which cause its black appearance in hand specimen. The natural alteration of phlogopite to vermiculite and talc takes place in alkaline. Na-rich rocks by hydration and losses of anions and cations from the interlayer and from the tetrahedral and octahedral layers, and by relative increase of Si and Mg.

Natural alteration of phlogopite to vermiculite. In addition to hydration which accompanies losses of the interlayer K and Na, the phlogopite loses Al, Ti, Rb, Fe, Mn, F and Cl (Table 1). The above losses of cations and anions are compensated by relative increases of Si, Mg and H_2O. However, the increased silica content is insufficient to compensate for the loss of alumina which results in a Si–Al-deficient tetrahedral layer and its unusual composition, or in vacant tetrahedral positions. The proportions of fluorine lost exceeds that of chlorine, as already observed in Example IVa. General chemical trends during natural alteration of phlogopite 'Ph' to vermiculite 'V' are similar to those observed in example IIe (not shown) when phlogopite alters to bright-green chlorite by losing K, Al, Ti, and gaining Mg. However, the bright-green chlorite gains also Fe and during the initial stage of alteration, loses some of its Si. The main difference between reactions in example IIc and V is in the behaviour of iron: in the green, partly altered phlogopite RT-866 'B' iron increases and is fixed in the structure, whereas in vermiculite 'V', iron decreases and is removed.

Natural alteration of phlogopite-vermiculite intergrowths to talc. During the natural alteration to talc on 'slickenside' surfaces along rock-fractures, the vermiculitized phlogopite loses the interlayer cations, tetrahedral and octahedral Al, Ti and part of Fe, as well as F and Cl from the OH,O-sheets. Part of the interlayer water is also expelled from the vermiculite, but talc retains excess water or hydroxyl as a substitute for F and Cl, and possibly in hydroxide impurities which might be intergrown with talc. The presence of possible impurities in vermiculite 'V' and in talc 'T' is inferred by the Si-deficient tetrahedral layer and by a slight excess of the octahedral Mg. Although Si-content considerably increases in talc 'T', its quantity is insufficient to fill the tetrahedral positions. The tetrahedral layer in both vermiculite 'V' and talc 'T' has a peculiar composition, resulting from considerable losses of Al and insufficient increases of Si. In order to fill the apparent tetrahedral vacancies, part

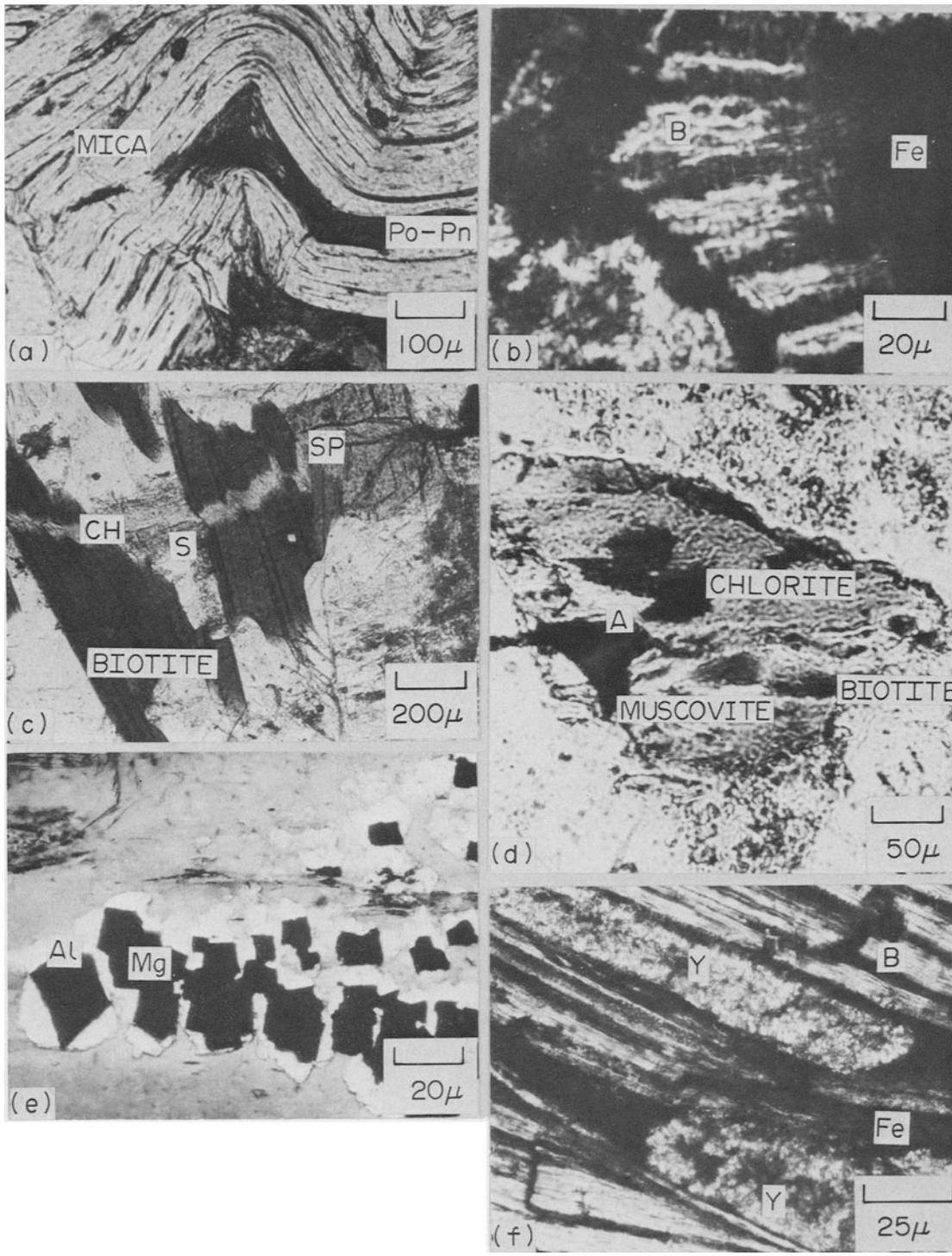

Fig. 1(a). Sulphide bands (Po=pyrrhotite; Pn=pentlandite) in a crenulated mica layer of fresh biotite schist RT-18.

1(b). Biotite (B) partly replaced by and coated with iron and uranium oxides in gneiss R-Kp-5.

1(c). Biotite flakes replaced by zig-zag veinlets of chlorite (CH) and serpentine (SP) and feldspar altered to sericite aggregates (S) along a fracture in greywacke RM-10.

1(d). Dark remnants of biotite in muscovite (white band) and residual chlorite (grey). The titania removed from the altered biotite crystallized as anatase (A) in gneiss R-Kp-5.

1(e). Magnetite (black) surrounded by secondary albite (white) in lepidomelane NEB-1.

1(f). Biotite bands (B) partly replaced by 'Ni-goethite' (Fe) and jarosite (Y) in oxidised portion of biotite schist RT-18.

https://doi.org/10.1346/CCMN.1975.0230312 Published online by Cambridge University Press

of Mg ions were placed into the tetrahedral layer, in addition to all Fe and Ti. Although they may be present, no Mg-rich minerals, such as serpentine and brucite, were observed on x-ray diffraction pattern.

SUMMARY AND CONCLUSIONS

The study was concerned mainly with intermediate alteration products containing various proportions of fresh mica remnants in intergrowths with the residual alteration phases, identified by the x-ray analysis. Results of this study provide data on diverse stages of alteration of mica in solid rocks; on remobilization of anions and cations during the alteration (Table 1); and on chemical compositions of the original micas and their residual alteration products, chlorites, serpentine, vermiculite and talc which form by pseudomorphous replacement of the micas. Quantities of released and gained constituents during various stages of alteration can be calculated. Thus, during alteration of 20% biotite to chlorite, 1 kg of mica schist RM-10 releases 20 g K; 25 g Si; 0·5 g Ti; 0·1 g F; 50 ppm Rb which are accompanied by apparent gains of 50 g OH; 1·5 g Al and 2·5 g Mg (Example IVa). Some of the released cations are removed from the host rock, while the others may be fixed in newly-formed secondary minerals.

Chemical composition of the residual chlorites depends on the chemical composition of the original mica, on the type of the host rock and on physico-chemical environment during alteration. In ultrabasic rocks the phlogopite alters to chlorite which has predominantly antigorite–ferroantigorite composition at the initial stage, and to talc at the advanced stage, by apparent gains of Si and Mg. In Si–Al-rich rocks, the residual chlorites usually contain more Al than the host micas and variable proportions of increased Mg and Fe which are fixed in the chlorite depending on the local distribution and availability of these ions due to decomposition of associated feldspars and Fe-rich sulphides. In the oxidation zone of a Fe–Ni-sulphide deposit, the goethite-, hematite- and jarosite-coated biotite alters to silica-rich amorphous flakes by losing different proportions of all the other constituents.

Results of this study contribute to scarce data on chemically-determined natural alteration reactions in solid rocks. The analyses obtained on fresh and altered portions of micas (Table 1 and structural formulae) indicate that alteration and hydration of micas involve losses and substitutions in the interlayer, in the octahedral and tetrahedral layers, and in the OH,O-sheets, in additions to the replacement of alkalis by hydroxides in the interlayer. Chemically complex biotites commonly alter to less complex oxides and hydrous silicates.

Acknowledgements—The author wishes to thank the Staff of the following mining companies for valuable suggestions and assistance with selection of sampling sites: Cominco Limited; Consolidated Canadian Faraday Limited; Falconbridge Nickel Mines Limited; and the International Nickel Company of Canada Limited. Electron microprobe analyses by G. R. Lachance and chemical analyses by J. L. Bouvier, both of the Central Laboratories and Technical Services Division, Geological Survey of Canada, and critical reading by J. L. Jambor of the Regional and Economic Geology Division, Geological Survey of Canada, are gratefully acknowledged.

REFERENCES

Buchan, R. and Blowes, J. H. (1968) Geology and mineralogy of a millerite nickel ore deposit, Marbridge No. 2 mine, Malartic, Quebec: *Can. Min. Met. Bull.* 1–6.

Carlson, H. D. (1958) Geology of the Werner Lake–Rex Lake area: Ontario Department Mines Report 66, pt. 4.

Dawson, K. R. (1966) A comprehensive study of the Preissac–Lacorne batholith, Abitiby county, Quebec: *Geol. Surv. Can. Bull.* **142.**

Hoda, S. N. and Hood, W. C. (1972) Laboratory alteration of trioctahedral micas: *Clays and Clay Minerals* **20,** 243–258.

Farmer, V. C., Russell, J. D., McHardy, W. J., Newman, A. C. D., Ahlrichs, J. L. and Rimsaite, J. Y. H. (1971) Evidence for loss of protons and octahedral iron from oxidized biotites and vermiculites: *Mineral. Mag.* **38,** 121–137.

Lachance, G. R. and Plant, A. G. (1973) Quantitative electron microprobe analysis using an energy dispersive spectrometer: *Geol. Surv. Can.* Paper 73–1, part B, 8–9.

Maxwell, J. A. (1968) *Rock and Mineral Analysis.* Interscience-Wiley, New York.

Mehmel, M. (1938) Ab- und Umbau am Biotit: *Chem. d. Erde* **11,** 307–332.

Rimsaite, J. (1967a) Biotite intermediate between dioctahedral and trioctahedral micas: *Clays and Clay Minerals* **15,** 375–393.

Rimsaite, J. (1967b) Studies of rock-forming micas: *Geol. Surv. Can. Bull.* **149.**

Rimsaite, J. (1970) Structural formulae of oxidized and hydroxyl-deficient micas and decomposition of the hydroxyl group: *Contr. Miner. Petrol.* **25,** 225–240.

Rimsaite, J. (1973a) Mica group minerals and related silicates in Canadian mineral deposits: *Geol. Surv. Can.* Paper 73–1. part B, 205–209.

Rimsaite, J. (1973b) Genesis of chlorite, vermiculite, serpentine and secondary oxides in ultrabasic rocks: *Proc. Int. Clay Conf.* 1972, Madrid, Spain, 291–302.

Robert, M. and Pedro, G. (1973) Etablissement d'un schema de l'evolution experimentale des micas trioctaedriques en fonction des conditions du milieu (pH concentration): *Proc. Int. Clay Conf.* 1972, Madrid, Spain, 433–447.

Zurbrigg, H. F. (1963) Thompson mine geology: *Can. Inst. Mining Met. Bull.* **56,** 451–460.